# Interaction of glutamic-acid-rich proteins with the cGMP signalling pathway in rod photoreceptors

**Heinz G. Körschen*, Michael Beyermann†, Frank Müller*, Martin Heck‡, Marius Vantler*, Karl-Wilhelm Koch*, Roland Kellner‖§, Uwe Wolfrum‖¶, Christian Bode‖¶, Klaus Peter Hofmann‡ & U. Benjamin Kaupp***

* *Institut für Biologische Informationsverarbeitung, Forschungszentrum Jülich, 52425 Jülich, Germany*
† *Forschungsinstitut für Molekulare Pharmakologie, 10315 Berlin, Germany*
‡ *Institut für Medizinische Physik und Biophysik, Universitätsklinikum Charité, Humboldt-Universität, 10998 Berlin, Germany*
§ *Institut für Physiologische Chemie und Pathobiochemie, Universität Mainz, 55099 Mainz, Germany*
¶ *Institut für Zoologie, Universität Karlsruhe, 76128 Karlsruhe, Germany*

**The assembly of signalling molecules into macromolecular complexes (transducisomes) provides specificity, sensitivity and speed in intracellular signalling pathways[1,2]. Rod photoreceptors in the eye contain an unusual set of glutamic-acid-rich proteins (GARPs) of unknown function[3–7]. GARPs exist as two soluble forms, GARP1 and GARP2, and as a large cytoplasmic domain (GARP′ part) of the β-subunit of the cyclic GMP-gated channel[3–7]. Here we identify GARPs as multivalent proteins that interact with the key players of cGMP signalling, phosphodiesterase and guanylate cyclase, and with a retina-specific ATP-binding cassette transporter (ABCR)[8,9], through four, short, repetitive sequences. In electron micrographs, GARPs are restricted to the rim region and incisures of discs in close proximity to the guanylate cyclase and ABCR, whereas the phosphodiesterase is randomly distributed. GARP2, the most abundant splice form, associates more strongly with light-activated than with inactive phosphodiesterase, and GARP2 potently inhibits phosphodiesterase activity. Thus, the GARPs organize a dynamic protein complex near the disc rim that may control cGMP turnover and possibly other light-dependent processes. Because there are no similar GARPs in cones, we propose that GARPs may prevent unnecessary cGMP turnover during daylight, when rods are held in saturation by the relatively high light levels.**

The β-subunit of the cGMP-gated channel has a unique bipartite structure[4]; it embodies a membrane-spanning region (β′ part) and a large cytosolic amino-terminal region (GARP′ part) (Fig. 1a). The β′ part contains all the functional motifs characteristic of cGMP-gated channel subunits, whereas the GARP′ part is largely identical with a soluble splice form, GARP1 (refs 3, 4). Another splice form, GARP2, lacks the carboxy-terminal glutamic-acid-rich region[5,6] (Fig. 1a).

We found that antibodies, each specific for one GARP form (see epitopes in Fig. 1a), recognized polypeptides with a relative molecular mass ($M_r$) of ~240,000 (240K; channel β), 130K (GARP1) and 62K (GARP2), respectively, in western blots of rod outer segments (ROS) (Fig. 1b). The differences between the calculated and apparent $M_r$s of GARPs result from the anomalous electrophoretic mobility caused by the large number of Glu residues, which reduce SDS binding[4]. A comparison of the staining intensity produced by a common anti-GARP antibody suggests that GARP2 is much more abundant than GARP1 (Fig. 1b; see also ref. 6). Moreover, by comparing the staining intensity of the 62K band with that of known amounts of recombinant GARP2 (rGARP2), we estimate that GARP2 is at least as abundant as phosphodiesterase (Rh: GARP2 ≈ 100 : 1; data not shown). Thus, GARP2 is a major protein of ROS. We separated ROS proteins into soluble and membrane fractions, and tested for the presence of GARPs by western blotting. Hypotonic washing resulted in the loss of GARP1 and GARP2 from the membrane fraction and complete recovery in the soluble fraction (Fig. 1c; compare lanes HMF and HSF). In contrast, isotonic washing did not remove GARPs from membranes (compare lanes IMF and ISF). Under isotonic conditions, soluble GARP1 and GARP2 completely reassociate with membranes depleted of both proteins (Fig. 1c; compare lanes RMF and RSF). Thus, like transducin and phosphodiesterase, GARP1 and GARP2 are tightly bound to the membrane at physiological conditions.

In vertical cryosections of bovine retina (Fig. 1d), anti-GARP stained outer segments and spherules of rods (Fig. 1d, arrowheads), but not other retinal cells, including cone photoreceptors. This finding was corroborated using freshly dissociated rods and cones. Whereas the outer segment and spherule of solitary rods were labelled (Fig. 1e), we detected no staining in any compartment of solitary cones (Fig. 1f, arrowhead). This indicates that GARPs may have a function that is specific to rods and absent in cones, although it is possible that cones express distantly related GARPs not recognized by the antibodies.

The common N-terminal region of GARPs contains four consecutive proline-rich repeats, R1–R4 (Fig. 1g). The repeat motif is characterized by an invariant Trp residue and a Pro–Gln–Pro triplet separated by nine, mostly conserved, residues, except that the first repeat is shorter than the others. Because R1–R4 are the most conserved sequence elements among GARPs from different species[3–7], we reasoned that these repeats serve as targets for binding other proteins. To identify potential target proteins, we constructed affinity columns from peptides, each representing one of the four repeats. ROS proteins were separated into cytosolic and membrane fractions and tested for their ability to bind to the peptide columns (Fig. 2). Phosphodiesterase (α, β; 90K) is the most abundant cytosolic protein retained by the columns, then eluted by SDS buffer (Fig. 2a). The 37K α-subunit ($T_\alpha$) (Fig. 2a) and the 35K β-subunit ($T_\beta$) (data not shown) of transducin bound weakly to repeat columns, while GARP1 (130K) and GARP2 (62K) bound quantitatively (Fig. 2a). Polypeptide binding to R1–R4 was specific; binding to an unrelated peptide or an empty column was absent or insignificant (Fig. 2a, lanes C1, C2). Binding was also specific inasmuch as other proteins, for example protein kinase C (Fig. 2a), recoverin or arrestin (data not shown), did not bind to the columns.

When we used stripped, detergent-solubilized ROS membranes, polypeptides of $M_r$s 63K, 112K, 220K and 240K bound to the columns. The 63K and 240K polypeptides have been identified as the α- and β-subunit, respectively, of the rod cGMP-gated channel (Fig. 2b), the 112K polypeptide as guanylate cyclase (Fig. 2b) and the 220K polypeptide as ABCR[8–10]. Rhodopsin, the most abundant protein, did not specifically bind to the R1–R4 peptides. The repeats are not equal in their potency in binding target proteins. For example, R2 and R3 bind phosphodiesterase strongly, whereas R1 and phosphodiesterase interact weakly, if at all (Fig. 2a). However, we found no consistent pattern of target preference to suggest that each repeat recruits a specific protein, as has been found for PDZ domains in the InaD scaffolding protein of *Drosophila* photoreceptors[1,11]. Thus, more than one repeat or the tetrad repeat unit might be involved in binding target proteins.

Using purified components, we examined the possibility that some proteins do not bind on their own, but instead are associated with other target proteins. The purified forms of phosphodiesterase, rGARP2, $T_\alpha$, $T_{\beta\gamma}$ and holo-$T_{\alpha\beta\gamma}$ tended to undergo hydrophobic

‖ Present addresses: Biomedizinische Forschung, Merck AG, 64271 Darmstadt, Germany (R.K.); Institut für Zoologie, Universität Mainz, 55099 Mainz, Germany (U.W., C.B.)

interactions with the column matrix (data not shown). Small amounts of detergents reduced non-specific binding of phosphodiesterase and rGARP2 to control columns, while preserving binding to R3 (Fig. 2c); therefore, phosphodiesterase and rGARP2 interact directly with R3. In contrast, detergent abolished binding of $T_\alpha$ and $T_{\alpha\beta\gamma}$ to both R3 and control columns (shown for $T_\alpha$ in Fig. 2c). This result, along with the gel-filtration experiment (see below), implies that transducin interacts, at most, only weakly with GARP repeats. The purified cGMP-gated channel, consisting of α- and β-subunits[4], bound to R3 but not to the control peptide (Fig. 2c). A dodecyl maltoside extract of ROS membranes[12] highly enriched in guanylate cyclase also contained tubulin and actin, but no ABCR or cGMP-gated channel or rhodopsin (ref. 13; and data not shown). The guanylate cyclase was completely removed from the extract (Fig. 2c) by the R3 column, along with tubulin and actin (data not shown) but not by a control. This demonstrates that cytoskeletal elements participate in a complex involving guanylate cyclase[13] and GARPs. Purified target proteins also bound to R2, but not to 'scrambled' R2 (having the same amino-acid composition as R2, but in random sequence; data not shown).

We used a complementary approach to demonstrate a high-affinity complex between native GARPs and phosphodiesterase. Soluble ROS proteins were fractionated by gel filtration and the elution profiles of phosphodiesterase and GARPs were analysed by western blotting (Fig. 2d). In a cytosolic extract of illuminated ROS, most GARP2 almost perfectly co-elutes with phosphodiesterase in two column fractions that predict a $M_r$ of ~230–270K for the complex, whereas a smaller portion of GARP2 elutes in column fractions compatible with a monomer (~30K) and a dimer (~60K). For an extract prepared in the dark, the elution profile is shifted towards the monomeric/dimeric forms of GARP2 (Fig. 2d). These results show that GARP2 is in binding equilibrium with a high-affinity phosphodiesterase/GARP2 complex and that active phosphodiesterase displays a higher affinity for GARP2 than does holo-phosphodiesterase.

Therefore, we examined whether GARP2 affects phosphodiesterase activity. Recombinant GARP2 up to concentrations of 5 μM did not affect the basal activity of purified phosphodiesterase (Fig. 3a). Phosphodiesterase activation by purified $T_\alpha$–GTPγS (molar ratio phosphodiesterase: $T_\alpha$ = 1 : 8, hydrolysis turnover 200–320 cGMP molecules $s^{-1}$) was inhibited by rGARP2 to almost basal levels (10–20%), with 50% inhibitory concentration of roughly 10 nM (Fig. 3a). In contrast, the activity of trypsinized phos-

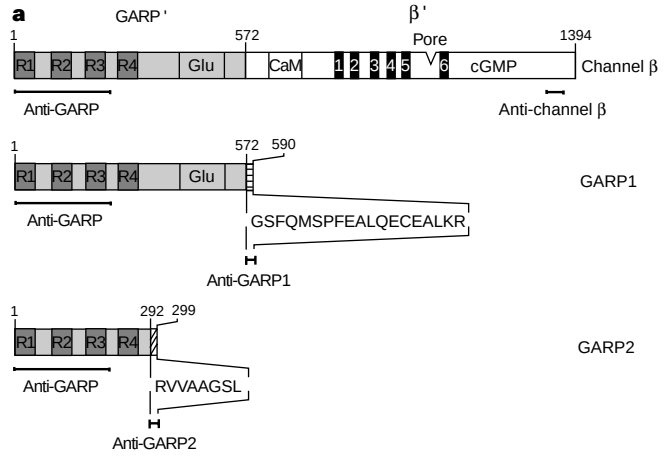


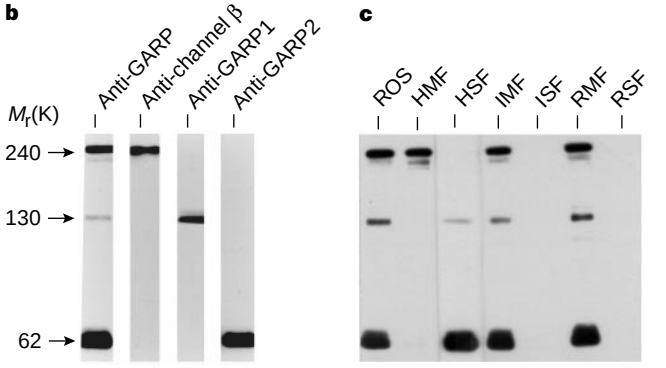


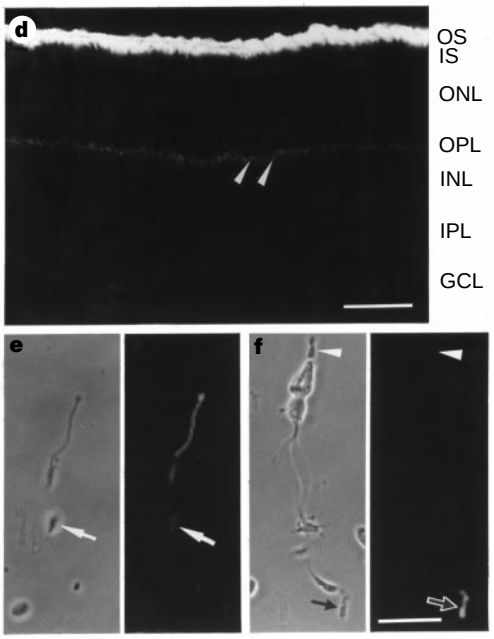



**Figure 1** Structural features of GARPs and localization to rod photoreceptors. **a**, Diagram of GARP1, GARP2 and the β-subunit of the cGMP-gated channel, highlighting the four repeats (R1–R4), the glutamic-acid-rich region (Glu), a calmodulin-binding site (CaM), the transmembrane segments (1–6), the pore region and the binding site for cGMP. **b**, Immunoblots showing the size and relative abundance of the three GARP polypeptides in ROS. Western blot (5 μg rhodopsin) was probed with antibodies specific for GARP1 (anti-GARP1), GARP2 (anti-GARP2), the β subunit (anti-channel β) and all three GARP polypeptides (anti-GARP). The epitopes against which antibodies were directed are shown in **a**. **c**, Membrane association of GARPs. Western blot was probed with the anti-GARP antibody. HMF, hypotonic membrane fraction; HSF, hypotonic soluble fraction; IMF, isotonic membrane fraction; ISF, isotonic soluble fraction; RMF, reconstituted membrane fraction; RSF, reconstituted soluble fraction. Samples contained roughly 5 μg rhodopsin. **d**, Vertical section of the bovine retina stained with antibody Anti-GARP. Rod outer segments (OS) and rod spherules in the outer plexiform layer (OPL, arrowheads) are labelled. GCL, ganglion cell layer; INL, inner nuclear layer; IPL, inner plexiform layer; IS, inner segment; ONL, outer nuclear layer. **e**, Isolated rod photoreceptor shown in phase contrast (left) and under epifluorescence (right). **f**, No staining is found in an isolated cone; the arrowhead marks the cone OS, the arrow points to a nearby rod OS that is labelled. Scale bars: 50 μm (**d**); 20 μm (**e**, **f**). **g**, Amino-acid alignment of R1–R4 from bovine GARPs. Black boxes indicate amino-acid identities; grey boxes show conservative substitutions.

phodiesterase was not inhibited; if anything, activity increased slightly at high rGARP2 concentrations (Fig. 3a), suggesting that inhibition by GARP2 requires the phosphodiesterase γ-subunit that is degraded by trypsin and/or $T_\alpha$–GTPγS. We obtained similar results with partially purified native GARP2. In rod photoreceptors, light activates phosphodiesterase on the surface of the disc membrane. To mimic this situation, we used a near-infrared light-scattering signal[14] to monitor the activation of membrane-bound phosphodiesterase by light. The 'phosphodiesterase signal' was progressively attenuated by increasing amounts of rGARP2 (Fig. 3b). The fraction of the signal that could be maximally suppressed varied between protein preparations, but was usually 50–80%. Thus, rGARP2 inhibits both soluble and membrane-bound phosphodiesterase.

The ABCR[8,9] (also called the rim protein[10]) and guanylate cyclase[15] lie at the disc margins. The identification of R1–R4 as

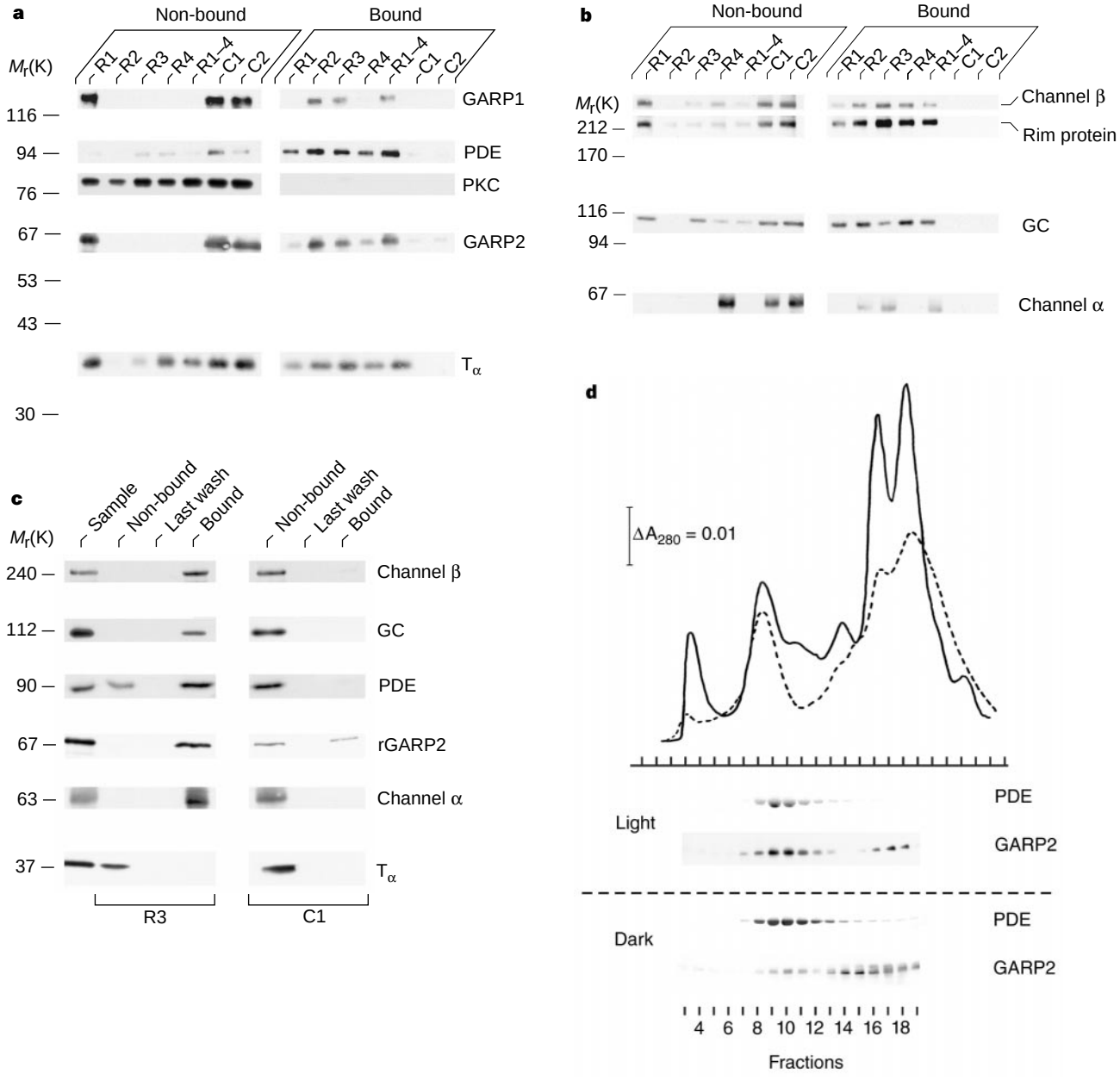


**Figure 2** Association of rod outer segment proteins with GARPs. Analysis of binding to GARP repeats R1–R4 by affinity chromatography with soluble proteins (**a**), membrane proteins (**b**) and purified components (**c**). **a**, Western-blot analysis of bound and non-bound column fractions of cytosolic proteins using the following antibodies: polyclonal anti-GARP; polyclonal α′-III, specific for phosphodiesterase (a gift from J. Beavo) monoclonal 3, specific for the α-subunit of protein kinase C (PKC; Transduction Laboratories); and $G_{\alpha\text{-t}}$ (K-20), specific for $T_\alpha$ (Santa Cruz Biotechnology). Columns either carried a single repeat (R1, R2, R3, R4) or a mixture of the four repeats (R1–R4), or, as controls, an unrelated peptide (C1) or no peptide (empty column) (C2). **b**, Western-blot analysis bound and non-bound column fractions of integral membrane proteins using the following antibodies: polyclonal anti-channel β (PPc32K in ref. 4), specific for the β-subunit; polyclonal FPc39K, specific for the α-subunit of the channel; polyclonal ABCR2374, specific for the ABC transporter (a gift from J. Nathans); and polyclonal PPc3, specific for guanylate cyclase (GC). **c**, Affinity chromatography of purified proteins with immobilized R3 and control columns (see Methods). Western-blot signals of the sample input that had been applied to the column (Sample), of the non-bound fraction (Non-bound), the last-wash fraction (Last wash) and the fraction eluted by SDS buffer (Bound). **d**, Gel-filtration chromatography on a Superdex-200 column of dark and light extracts of cytosolic proteins. Upper part, protein elution profile of light (continuous) and dark (dashed) extract (0.5-ml fractions) monitored at 280 nm. Lower part, proteins were visualized with Coomassie (PDE) and by western blot using anti-GARP antibody (GARP2).

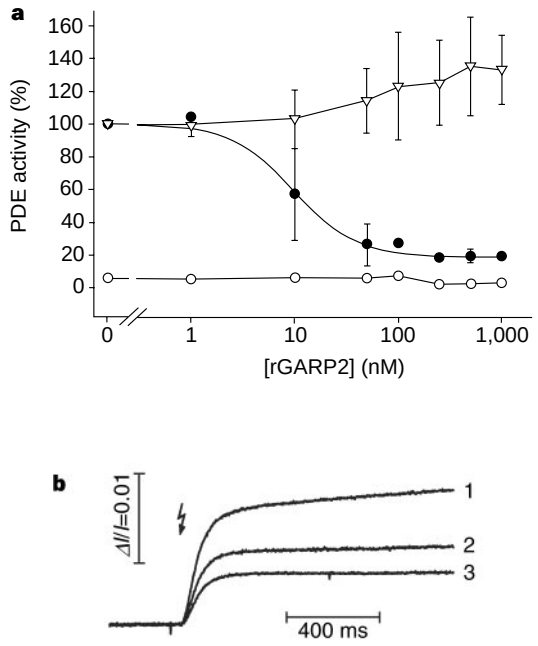


**Figure 3** Inhibition of phosphodiesterase (PDE) by rGARP2. **a**, Normalized PDE activity (%) as a function of rGARP2 concentration. Holo-PDE was activated either by $1.5 \times 10^{-7}$ M $T_{\alpha}$-GTP$\gamma$S (●) or by trypsinization (▽); ○, effect of rGARP2 on basal activity. PDE activity (turnover number $s^{-1}$) was normalized to the activity without the addition of rGARP2. Basal activity of holo-PDE was normalized to trypsinized PDE activity. Data represent means of at least three determinations ± s.d. **b**, Near-infrared light-scattering monitor of PDE activation by a light flash and inhibition by rGARP2; trace 1, 3 μM rhodopsin, 0.35 μM transducin, 0.2 μM PDE, 500 μM GTP, no rGARP2; trace 2, plus 0.2 μM rGARP2; trace 3, plus 0.6 μM rGARP2.

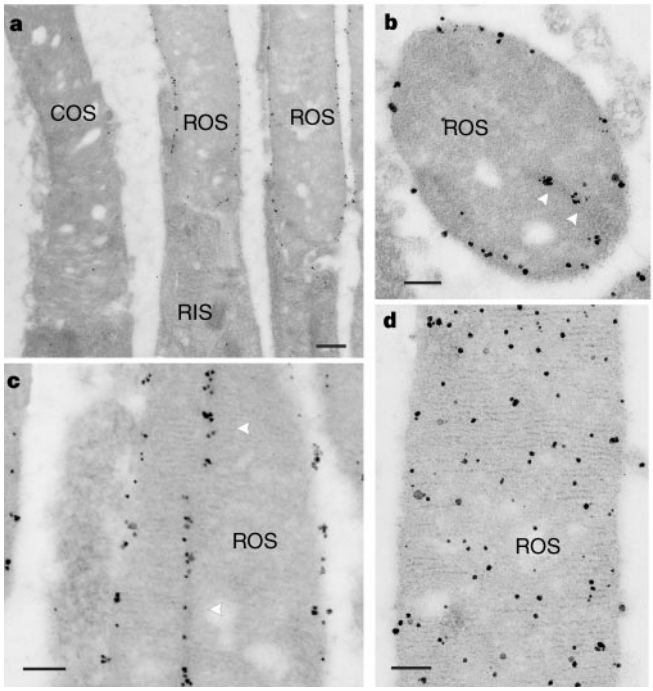


**Figure 4** Immunoelectron microscopic localization of GARPs and PDE in photoreceptor cells. **a**, Longitudinal section through bovine photoreceptor cells. Silver-enhanced immunogold labelling with anti-GARP is restricted to peripheral regions of ROS. Rod inner segments (RIS) and cone outer segments (COS) are not labelled. **b**, Transverse section; **c**, longitudinal section through bovine ROS. Silver-enhanced immunogold labelling with anti-GARP is present at peripheral regions and in incisures (arrowheads) of ROS. **d**, Electron micrograph of a longitudinal section through a ROS, illustrating silver-enhanced immunogold labelling of retinal PDE. The entire outer segment is labelled. Scale bars: **a**, 500 nm; **b–d**, 200 nm.

protein-recognition domains raises the possibility that GARPs act *in vivo* to assemble a protein complex at the disc rim, in close proximity to the cGMP-gated channel in the plasma membrane[16]. If GARP2 interacts with one or several of these membrane proteins, it should be predominantly located at the disc margin or the plasma membrane. We studied the subcellular distribution of GARPs by electron microscopy (Fig. 4). Silver-enhanced immunogold labelling with the anti-GARP antibody revealed that GARPs are localized exclusively at the circumference and incisures of rods in longitudinal and transverse sections of bovine ROS (Fig. 4a–c). Rod inner segments and cone outer segments were not labelled (Fig. 4a). Mammalian rods usually have a single incisure per disc[17] and incisures of adjacent discs are aligned for several micrometres along the outer segment. Several of these longitudinal clefts are laterally displaced[18]. Therefore, decoration of incisures similar to the pattern shown in Fig. 4c is typical for mammalian rods and is also observed for the ABCR[8]. These results demonstrate that all GARPs are restricted to the small subcellular space between the plasma membrane (GARP′ part) and disc rim (GARP1 and GARP2). In contrast, we observed uniform immunogold labelling of retinal phosphodiesterase throughout the outer segment (Fig. 4d). In control experiments, preincubation of the antibody with rGARP2 (1 mg $ml^{-1}$) entirely abolished ROS labelling, whereas preincubation with an unrelated recombinant protein (centrin 1) had no effect (data not shown).

In conclusion, we provide evidence that soluble GARPs are confined to the rim region and incisures of discs. Although the electron micrographs cannot prove a physical interaction, it is plausible that GARPs are confined to the rim by binding to guanylate cyclase and the ABCR, which also occur at the disc margins[8,10,15] (Fig. 5). The GARP′ part of the channel β-subunit, in principle, may also interact with the large cytoplasmic domains of guanylate cyclase and ABCR across the narrow gap between plasma and disc membrane (~10 nm; ref. 19). Co-immunoprecipitation experiments failed to demonstrate the existence of such a protein complex unequivocally (unpublished). However, solubilization of membrane proteins, in particular of guanylate cyclase, required high detergent concentrations that might have disrupted a complex between components of the plasma and disc membrane.

What is the function of GARPs? Active phosphodiesterase is turned off by the endogenous GTPase activity of $T_{\alpha}$–GTP involving RGS9 (ref. 20)—a member of the family of GAP proteins—and the β-subunit of type-5 G protein[21]. The powerful inhibition of active phosphodiesterase by rGARP2 suggests an independent mechanism of phosphodiesterase inactivation that might be important for termination and adaptation of the light response: active phosphodiesterase molecules that reach the disc rim by diffusion will be deactivated by GARP2 or the GARP′ part of the channel. An intriguing scenario is that the two inactivation mechanisms operate in different light regimes. Sequestration by GARPs may become the dominant inactivation mechanism at high light intensities, when it is highly probable that a significant fraction of active phosphodiesterase is reaching the disc margins[22]. In this respect, GARPs may organize an 'adaptational' signalling complex at the disc rim that downregulates the high cGMP turnover during daylight, when rod function is saturated. □

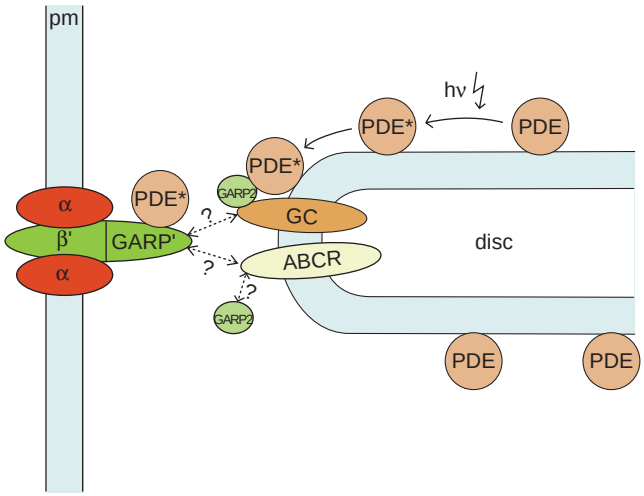


**Figure 5** Hypothetical model of protein interactions. In the dark, GARP2 is associated with the GC (and possibly ABCR) at the disc rim, whereas PDE is randomly distributed on the disc surface. On illumination, active PDE* reaching the disc rim competes with GC (or ABCR?) for GARP2 and thereby becomes inactivated. PDE* may also interact with the GARP′ part of the channel β-subunit. The GARP′ part and the cytoplasmic domains of GC and ABCR are sufficiently large to span the small cytoplasmic gap (~10 nm; ref. 19) between plasma membrane and disc rim. Whether such an interaction exists *in vivo* is unclear. GARP1 is only a minor component and has not been included. pm, plasma membrane.

## Methods

**Western blot and immunohistochemistry.** Polyclonal antibodies were produced and purified as described previously[4]. Antibody anti-GARP1 was raised against a peptide from the C terminus of GARP1 (amino acids 572–590); anti-GARP2 against a peptide from the C terminus of GARP2 (290–299); anti-GARP against a glutathione *S*-transferase fusion protein of the N-terminal sequence (5–221) common to GARP1, GARP2 and the GARP′ part of the rod cGMP-gated channel β-subunit. Western blotting was performed as described previously[4,23], as were immunohistochemistry and dissociation of interact photoreceptors from the retina[23].

**Association of GARPs with membranes.** ROS membranes were washed three times with either a hypotonic buffer (10 mM HEPES, 2 mM DTT, 2 mM EGTA at pH 7.4) or an isotonic buffer (plus 150 mM KCl). After each washing step, the suspension was centrifuged for 15 min at 100,000 r.p.m. (Beckman TLA 100). The membrane pellet obtained after three washing steps was called either the hypotonic (HMF) or isotonic (IMF) membrane fraction; the respective supernatants obtained after the first washing step were called hypotonic (HSF) or isotonic (ISF) soluble fractions. The reversibility of association of soluble GARPs with membranes was tested by 5 min incubation on ice of hypotonically washed membranes devoid of GARPs (HMF) with the soluble fraction which contained GARPs (HSF) under isotonic conditions, followed by centrifugation at 100,000 r.p.m. to yield the reconstituted membrane fraction (RMF) and reconstituted soluble fraction (RSF).

**Gel filtration.** Supernatants of hypotonically washed ROS were fractionated by gel-filtration chromatography on a Superdex-200 column (Pharmacia). Phosphodiesterase and GARPs were detected in elution fractions (0.5 ml) by western blotting using Coomassie staining (phosphodiesterase) and the anti-GARP antibody, respectively.

**Affinity-column chromatography.** The amide form of peptides was synthesized, purified and characterized as described elsewhere[24]. The sequences of peptides were: R1, MLGWVQRVLPQPPG; R2, GWVLTWLRKGVEKVVPQPAH; R3, PWLLRWFEQNLEKMLPQPPK; R4, ARLMAWILHRLEMALPQPV; and control peptides (C1) GEGRLKVLQE or 'scrambled' R2 (GHWAVPLQTPWVLVRKKEGV). Peptides were immobilized to activated CH Sepharose 4B by α-amino groups. Purified ROS were lysed and washed three times in buffer A (10 mM HEPES-KOH pH 7.4, 2 mM DTT). The supernatant from the lysis step was designated the cytosolic fraction, and the membrane pellet, stripped of all soluble proteins and solubilized in buffer A containing 15 mM CHAPS, was designated the membrane fraction. Affinity chromatography was performed in isotonic buffer B (150 mM KCl, 2 mM DTT, 0.2 mM PMSF) with the following additions: 20 mM Tris-HCl pH 8.0, 0.05% Tween 20 (purified transducin, recombinant GARP2); or 10 mM HEPES/KOH pH 7.4, 15 mM CHAPS (purified cGMP-gated channel, purified phosphodiesterase and ROS membrane fraction); or 10 mM HEPES/KOH pH 7.4 (ROS soluble fraction); or 20 mM Tris–HCl pH 8.0, 20 mM *N*-dodecyl maltoside (extract enriched in guanylate cyclase). Columns were washed four times with incubation buffer and twice with hypotonic buffer (no KCl). Bound proteins were eluted by Laemmli SDS buffer and analysed by western blotting. Purification of signalling components was as described for transducin and phosphodiesterase[14], guanylate cyclase[12] and rod cGMP-gated channel[25]. Recombinant GARP2 (rGARP2) was obtained by expression as fusion protein using a pET30a vector (Novagen) and purification with a Ni-chelate column.

**Phosphodiesterase assay.** Purified phosphodiesterase was preincubated in a final volume of 50 μl with $T_\alpha$–GTPγS and various rGARP2 concentrations in a buffer containing 200 mM NaCl, 10 mM HEPES pH 7.4, 2 mM DTT, 2 mM $MgCl_2$ for 10 min at 25 °C. The concentration of holo-phosphodiesterase was $1.75 \times 10^{-8}$ M and that of trypsinized phosphodiesterase was $2 \times 10^{-9}$ M. The reaction was started by adding 500 μM cGMP and was stopped after 20 s by adding 50 μl ice-cold 100 mM EDTA and boiling for 5 min. The cGMP and 5′-GMP concentrations were analysed by HPLC using a nucleotide separation and quantification system as described elsewhere[26].

**Real-time light-scattering assay.** Changes in light-induced near-infrared light scattering of membrane suspensions that have been reconstituted with purified transducin and phosphodiesterase were measured as described previously[14].

**Electron microscopy.** Immunoelectron microscopy was performed with LR White sections of isolated bovine retinae as described[27,28] previously. Nanogold (Nanoprobes, Stony Brook) labelling of ultra-thin sections was silver-enhanced as described[29] and examined in a Zeiss EM 912Ω electron microscope.

Received 6 April; accepted 14 June 1999.


1. Tsunoda, S. *et al.* A multivalent PDZ-domain protein assembles signalling complexes in a G-protein-coupled cascade. *Nature* **388,** 243–249 (1997).
2. Zuker, C. S. & Ranganathan, R. The path to specificity. *Science* **283,** 650–651 (1999).
3. Sugimoto, Y., Yatsunami, K., Tsujimoto, M., Khorana, H. G. & Ichikawa, A. The amino acid sequence of a glutamic acid-rich protein from bovine retina as deduced from the cDNA sequence. *Proc. Natl Acad. Sci. USA* **88,** 3116–3119 (1991).
4. Körschen, H. G. *et al.* A 240 kDa protein represents the complete β subunit of the cyclic nucleotide-gated channel from rod photoreceptor. *Neuron* **15,** 627–636 (1995).
5. Ardell, M. D. *et al.* cDNA, gene structure, and chromosomal localization of human GAR1 (CNCG3L), a homolog of the third subunit of bovine photoreceptor cGMP-gated channel. *Genomics* **28,** 32–38 (1995).
6. Colville, C. A. & Molday, R. S. Primary structure and expression of the human β-subunit and related proteins of the rod photoreceptor cGMP-gated channel. *J. Biol. Chem.* **271,** 32968–32974 (1996).
7. Grunwald, M. E., Yu, W.-P., Yu, H.-H. & Yau, K.-W. Identification of a domain on the β-subunit of the rod cGMP-gated cation channel that mediates inhibition by calcium–calmodulin. *J. Biol. Chem.* **273,** 9148–9157 (1998).
8. Illing, M., Molday, L. L. & Molday, R. S. The 220-kDa rim protein of retinal rod outer segment is a member of the ABC transporter superfamily. *J. Biol. Chem.* **272,** 10303–10310 (1997).
9. Allikmets, R. *et al.* A photoreceptor cell-specific ATP-binding transporter gene (*ABCR*) is mutated in recessive Stargardt macular dystrophy. *Nature Genet.* **15,** 236–246 (1997).
10. Papermaster, D. S., Schneider, B. G., Zorn, M. A. & Kraehenbuhl, J. P. Immunocytochemical localization of a large intrinsic membrane protein to the incisures and margins of frog rod outer segment disks. *J. Cell Biol.* **78,** 415–425 (1978).
11. Montell, C. TRP trapped in fly signaling web. *Curr. Opin. Neurobiol.* **8,** 389–397 (1998).
12. Koch, K.-W. & Lambrecht, H.-G. in *Signal Transduction in Photoreceptor Cells* (eds Hargrave, P. A., Hofmann, K. P. & Kaupp, U. B.) 259–267 (Springer, Berlin, 1992).
13. Schrem, A., Lange, C., Beyermann, M. & Koch, K.-W. Identification of a domain in guanylyl cyclase-activating protein 1 that interacts with a complex of guanylyl cyclase and tubulin in photoreceptors. *J. Biol. Chem.* **274,** 6244–6249 (1999).
14. Heck, M. & Hofmann, K. P. G-protein-effector coupling: A real-time light-scattering assay for transducin-phosphodiesterase interaction. *Biochemistry* **32,** 8220–8227 (1993).
15. Liu, X. *et al.* Ultrastructural localization of retinal guanylate cyclase in human and monkey retinas. *Exp. Eye Res.* **59,** 761–768 (1994).
16. Cook, N. J., Molday, L. L., Reid, D., Kaupp, U. B. & Molday, R. S. The cGMP-gated channel of bovine rod photoreceptors is localized exclusively in the plasma membrane. *J. Biol. Chem.* **264,** 6996–6999 (1989).
17. Pedler, C. M. & Tilly, R. The fine structure of photoreceptor discs. *Vision Res.* **7,** 829–836 (1967).
18. Eckmiller, M. S. & Toman, A. Association of kinesin with microtubules in diverse cytoskeletal systems in the outer segments of rods and cones. *Acta Anat.* **162,** 133–141 (1998).
19. Roof, D. J. & Heuser, J. E. Surfaces of rod photoreceptor disk membranes: Integral membrane components. *J. Cell Biol.* **95,** 487–500 (1982).

20. He, W., Cowan, C. W. & Wensel, T. G. RGS9, a GTPase accelerator for phototransduction. *Neuron* **20,** 95–102 (1998).
21. Makino, E. R., Handy, J. W., Li, T. & Arshavsky, V. Y. The GTPase activating factor for transducin in rod photoreceptors is the complex between RGS9 and type 5 G protein β subunit. *Proc. Natl Acad. Sci. USA* **96,** 1947–1952 (1999).
22. Pugh, E. N. Jr & Lamb, T. D. Amplification and kinetics of the activation steps in phototransduction. *Biochim. Biophys. Acta* **1141,** 111–149 (1993).
23. Bönigk, W. *et al.* Rod and cone photoreceptor cells express distinct genes for cGMP-gated channels. *Neuron* **10,** 865–877 (1993).
24. Zoche, M., Bienert, M., Beyermann, M. & Koch, K.-W. Distinct molecular recognition of calmodulin-binding sites in the neuronal and macrophage nitric oxide synthases: A surface plasmon resonance study. *Biochemistry* **35,** 8742–8747 (1996).
25. Hsu, Y.-T. & Molday, R. S. Modulation of the cGMP-gated channel of rod photoreceptor cells by calmodulin. *Nature* **361,** 76–79 (1993).
26. Lambrecht, H.-G. & Koch, K.-W. A 26 kd calcium binding protein from bovine rod outer segments as modulator of photoreceptor guanylate cyclase. *EMBO J.* **10,** 793–798 (1991).
27. Wolfrum, U. Centrin in the photoreceptor cells of mammalian retinae. *Cell Motil. Cytoskel.* **32,** 55–64 (1995).
28. Wolfrum, U., Liu, X., Schmitt, A., Udovichenko, I. P. & Williams, D. S. Myosin VIIa as a common component of cilia and microvilli. *Cell Motil. Cytoskel.* **40,** 261–271 (1998).
29. Danscher, G. Localization of gold in biological tissue. A photochemical method for light and electron microscopy. *Histochemistry* **71,** 81–88 (1981).

**Acknowledgements.** We thank J. Beavo, J. Nathans, I. Weyand and D. Weitz for antibodies, A. Eckert for preparing the manuscript, I. Weyand and R. Seifert for critical reading of the manuscript, and E. Pugh and R. Cote for discussions. This work was supported by grants from the EU (U.B.K.), the Deutsche Forschungsgemeinschaft (M.B., K.P.H., K.-W.K., U.B.K., U.W.) and the FAUN-Stiftung (U.W.).

Correspondence and requests for materials should be addressed to U.B.K. (e-mail: a.eckert@fz-juelich.de).

# Increased affiliative response to vasopressin in mice expressing the $V_{1a}$ receptor from a monogamous vole

**Larry J. Young*, Roger Nilsen*, Katrina G. Waymire†, Grant R. MacGregor† & Thomas R. Insel***

* *Department of Psychiatry and Behavioural Sciences and † Center for Molecular Medicine, Emory University, Atlanta, Georgia 30322, USA*

**Arginine vasopressin influences male reproductive and social behaviours in several vertebrate taxa[1] through its actions at the $V_{1a}$ receptor in the brain. The neuroanatomical distribution of vasopressin $V_{1a}$ receptors varies greatly between species with different forms of social organization[2,3]. Here we show that centrally administered arginine vasopressin increases affiliative behaviour in the highly social, monogamous prairie vole, but not in the relatively asocial, promiscuous montane vole. Molecular analyses indicate that gene duplication and/or changes in promoter structure of the prairie vole receptor gene may contribute to the species differences in vasopressin-receptor expression. We further show that mice that are transgenic for the prairie vole receptor gene have a neuroanatomical pattern of receptor binding that is similar to that of the prairie vole, and exhibit increased affiliative behaviour after injection with arginine vasopressin. These data indicate that the pattern of $V_{1a}$-receptor gene expression in the brain may be functionally associated with species-typical social behaviours in male vertebrates.**

Arginine vasopressin (AVP) and its non-mammalian homologue, arginine vasotocin (AVT), are involved in many species-typical, male social behaviours, including communication[4–7], aggression[4–6], sexual behaviour[7] and, in monogamous species, pairbonding and paternal care[8]. Pharmacological studies using selective antagonists indicate that the behavioural effects of AVP are mediated by the $V_{1a}$ receptor[8,9]. The $V_{1a}$ receptor is a member of a family of evolutionarily related receptors for the neurohypophysial peptides, arginine vasopressin and oxytocin, which includes the $V_{1a}$, $V_{1b}$, $V_2$ and oxytocin receptors, all of which are G-protein-coupled proteins comprising seven transmembrane domains[10]. The $V_{1a}$ receptor is exceptional in that its pattern of expression in the brain is phylogenetically plastic, with the neuroanatomical distribution of this receptor being unique in virtually every species examined[10].

Voles provide a useful model to test the relationship between receptor expression patterns and social behaviour. Prairie voles (*Microtus ochrogaster*) are highly affiliative, biparental and monogamous; whereas montane voles (*Microtus montanus*) are relatively asocial, non-paternal, and promiscuous[11]. In the male prairie vole, cohabitation and/or mating with a female stimulates both the central release of AVP[12,13] and the development of a pairbond and paternal care[8,12]. Central blockade of the vasopressin receptors during mating with a selective $V_{1a}$ antagonist prevents the normal development of pairbonds between mates and paternal care in male prairie voles[8,14]. Prairie and montane voles have strikingly different distributions of $V_{1a}$-receptor binding in the brain (Fig. 1a). We tested the hypothesis that these differences in $V_{1a}$-receptor binding patterns would confer species differences in behavioural response to AVP. Using an ovariectomized stimulus female placed in one side of a two-chambered arena, 2 ng of AVP delivered by intracerebroventricular (i.c.v.) injection to male prairie voles resulted in a significant increase in affiliative behaviour (olfactory investigation and grooming) toward the stimulus female ($P < 0.01$) (Fig. 1b). In contrast, the identical treatment had no effect on affiliative behaviour, compared with control injections, in male montane voles.

To investigate the mechanisms of the species differences in regional gene expression, we compared the structures of the prairie and montane vole $V_{1a}$-receptor genes, including the 5′ flanking regions (Fig. 2a). The $V_{1a}$-receptor gene encodes a protein of 420 amino-acid residues that is 99% homologous between the vole species. The binding kinetics of the receptor protein and its second messenger coupling are identical in both species[3]. Both 5′ and 3′ rapid amplification of complementary DNA ends (RACE) were used to identify the transcriptional boundaries of the gene (data not shown). The prairie vole $V_{1a}$ messenger RNA is composed of a 232-base-pair (bp) 5′ untranslated region (UTR), a 1,260-bp coding region followed by a 36-bp 3′ UTR. No CAAT or TATA enhancer

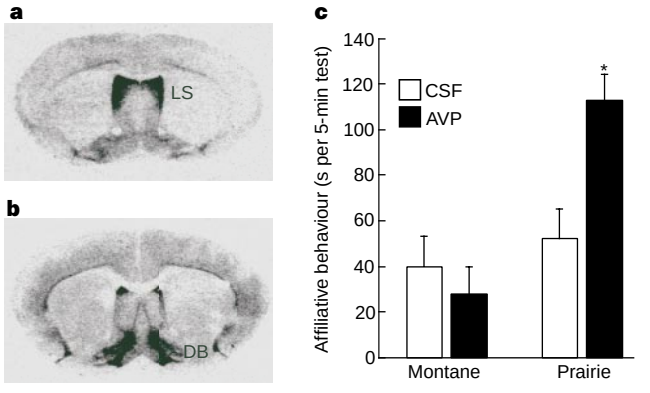


**Figure 1** Montane and prairie voles differ both in $V_{1a}$-receptor binding pattern and behavioural response to arginine vasopressin. Receptor autoradiography[6] illustrates the different patterns of $V_{1a}$-receptor binding in the brains of **a**, the non-monogamous montane vole, and **b**, the monogamous prairie vole. Note the high intensity of binding in the lateral septum (LS) of the montane vole but not the prairie vole, and in the diagonal band (DB) of the prairie vole but not the montane vole. Similar differences exist throughout the brain. **c**, Male prairie but not montane voles exhibit elevated levels of affiliative behaviour after vasopressin is administered directly into the brain (two-way ANOVA: species effect, $F(1,27) = 10.3$, $P < 0.01$; * Fisher's LSD post-hoc test, $P < 0.01$ compared with CSF-treated prairie voles).